University of Zurich[UZH]

Zurich Open Repository and Archive
University of Zurich
University Library
Strickhofstrasse 39
CH-8057 Zurich
www.zora.uzh.ch

Year: 2015

Insight into the beneficial immunomodulatory mechanism of the sevoflurane metabolite hexafluoro-2-propanol in a rat model of endotoxaemia

Urner, M ; Schläpfer, M ; Herrmann, I K ; Hasler, M ; Schimmer, R R ; Booy, C ; Roth Z'graggen, B ; Rehrauer, H ; Aigner, F ; Minshall, R D ; Stark, W J ; Beck-Schimmer, B

Abstract: Volatile anaesthetics such as sevoflurane attenuate inflammatory processes, thereby impacting patient outcome significantly. Their inhalative administration is, however, strictly limited to controlled environments such as operating theatres, and thus an intravenously injectable immunomodulatory drug would offer distinct advantages. As protective effects of volatile anaesthetics have been associated with the presence of trifluorinated carbon groups in their basic structure, in this study we investigated the water-soluble sevoflurane metabolite hexafluoro-2-propanol (HFIP) as a potential immunomodulatory drug in a rat model of endotoxic shock. Male Wistar rats were subjected to intravenous lipopolysaccharide (LPS) and thereafter were treated with HFIP. Plasma and tissue inflammatory mediators, neutrophil invasion, tissue damage and haemodynamic stability were the dedicated end-points. In an endotoxin-induced endothelial cell injury model, underlying mechanisms were elucidated using gene expression and gene reporter analyses. HFIP reduced the systemic inflammatory response significantly and decreased endotoxin-induced tissue damage. Additionally, the LPS-provoked drop in blood pressure of animals was resolved by HFIP treatment. Pathway analysis revealed that the observed attenuation of the inflammatory process was associated with reduced nuclear factor kappa B (NF- B) activation and suppression of its dependent transcripts. Taken together, intravenous administration of HFIP exerts promising immunomodulatory effects in endotoxaemic rats. The possibility of intravenous administration would overcome limitations of volatile anaesthetics, and thus HFIP might therefore represent an interesting future drug candidate for states of severe inflammation.

DOI: https://doi.org/10.1111/cei.12648

Posted at the Zurich Open Repository and Archive, University of Zurich
ZORA URL: https://doi.org/10.5167/uzh-113563
Journal Article
Accepted Version

Originally published at:
Urner, M; Schläpfer, M; Herrmann, I K; Hasler, M; Schimmer, R R; Booy, C; Roth Z'graggen, B; Rehrauer, H; Aigner, F; Minshall, R D; Stark, W J; Beck-Schimmer, B (2015). Insight into the beneficial immunomodulatory mechanism of the sevoflurane metabolite hexafluoro-2-propanol in a rat model of endotoxaemia. Clinical and Experimental Immunology, 181(3):468-479.
DOI: https://doi.org/10.1111/cei.12648

Insight into the beneficial immunomodulatory mechanism of the sevoflurane metabolite hexafluoro-2-propanol in a rat model of endotoxemia

Martin Urner, MD[1,2,*], Martin Schläpfer, MD MSc[1,2,*], Inge K. Herrmann, PhD[1,2], Melanie Hasler[1,2], Roman R. Schimmer[2], Christa Booy[1,2], Birgit Roth Z'graggen, PhD[1,2], Hubert Rehrauer, PhD[4], Richard D. Minshall, PhD [5], Wendelin J. Stark, PhD[3,X], and Beatrice Beck-Schimmer, MD[1,2,5,X,§]

[1] Institute of Anesthesiology, University Hospital Zurich, Rämistrasse 100, CH-8091 Zurich, Switzerland.

[2] Institute of Physiology, Zurich Center for Integrative Human Physiology, University of Zurich, Winterthurerstrasse 190, CH-8057 Zurich, Switzerland.

[3] Institute for Chemical and Bioengineering, Department of Chemistry and Applied Biosciences, ETH Zurich, 8093, Zurich, Switzerland.

[4] Functional Genomics Center Zurich, University of Zurich, Winterthurerstrasse 190, CH-8057 Zurich, Switzerland.

[5] University of Illinois, Department of Anesthesiology, 1740 West Taylor Street, Chicago, IL 60612

[*] These authors contributed equally to this work as first authors.
[X] These authors contributed equally to this work as senior authors.

Keywords: anesthesia; sepsis; inflammation; interleukin; fluorinated carbon groups
Short title: Hexafluoro-2-propanol in endotoxemic rats

Abbreviations: AnaConDa, Anesthetic Conserving Device; AP-1, activator protein-1; AST, aspartate transaminase; BALF, bronchoalveolar lavage fluid; BUN, blood urea nitrogen; BW, total body weight; CINC-1, cytokine-induced neutrophil chemoattractant-1; DAPI, diamidino-2-phenylindole; EGTA, ethylene glycol tetraacetic acid; ELISA, enzyme-linked immunosorbent assay; FiO2, fractional inspired oxygen concentration; HEPES, 4-(2-hydroxyethyl)-1-piperazineethanesulfonic acid; HFIP, hexafluoro-2-propanol; HMVEC, human microvascular endothelial cells; IKK, I kappa B kinases; IL-6, interleukin 6; IRAK 1/2, interleukin-1 receptor-associated kinase 1/2; LPS, lipopolysaccharide; MAP, arterial blood pressure; MCP-1, monocyte chemoattractant protein-1; NF-κB, nuclear factor-kappaB; NIK, NF-kappa-beta-inducing kinase = MAP3K14; PBS, phosphate-buffered saline; PKC, protein kinase C; PMA, phorbol-12-myristate-13-acetate; PMSF, phenylmethanesulfonylfluoride; TLR4, toll-like receptor 4; TNF-α, tumor necrosis factor-α; TRAF6, tumor necrosis factor (TNF) receptor-associated factor 6.

(§) Corresponding author:
Beatrice Beck-Schimmer, M.D.
University Hospital Zurich, Institute of Anesthesiology
Rämistrasse 100, CH-8091 Zurich, Switzerland
Phone: +41 44 255-2696, Fax: +41 44 255-4409
E-mail: beatrice.beckschimmer@uzh.ch

ABSTRACT

Volatile anesthetics such as sevoflurane attenuate inflammatory processes, thereby significantly impacting patient outcome. Their inhalative administration is, however, strictly limited to controlled environments such as operating theatres and thus an intravenously injectable immunomodulatory drug would offer distinct advantages. As protective effects of volatile anesthetics have been associated with the presence of trifluorinated carbon groups in their basic structure, we investigated in this study the water-soluble sevoflurane metabolite hexafluoro-2-propanol (HFIP) as a potential immunomodulatory drug in a rat model of endotoxic shock. Male Wistar rats were subjected to intravenous lipopolysaccharide (LPS) and thereafter were treated with HFIP. Endpoints were plasma and tissue inflammatory mediators, neutrophil invasion, tissue damage, and hemodynamic stability. In an endotoxin-induced endothelial cell injury model, underlying mechanisms were elucidated using gene expression and gene reporter analyses. HFIP significantly reduced the systemic inflammatory response and decreased endotoxin-induced tissue damage. Additionally, the LPS-provoked drop in blood pressure of animals was resolved by HFIP treatment. Pathway analysis revealed that the observed attenuation of the inflammatory process was associated with reduced NF-κB activation and suppression of its dependent transcripts. Taken together, intravenous administration of HFIP exerts promising immunomodulatory effects in endotoxemic rats. The possibility of intravenous administration would overcome limitations of volatile anesthetics and thus HFIP might therefore represent an interesting future drug candidate for states of severe inflammation.

INTRODUCTION

Sepsis accompanied by multiple organ failure is a leading cause of hospital morbidity and mortality in intensive care units (ICU) and is associated with tremendous financial costs [1]. The time elapsed until the focus of the infection is under control ultimately determines the fate of the patient [2]. Numerous supportive therapeutic strategies including early fluid resuscitation, microbial screening, and empiric antimicrobial therapy have been implemented to bridge the time to source control [3]. Volatile anesthetics provide beneficial effects in perioperative states of hypoxia-reoxygenation and ischemia-reperfusion injury [4, 5]. The improved outcome is accompanied by an altered immune response resulting in attenuation of the inflammatory response and tissue damage [6-9]. In recent work, the volatile anesthetic sevoflurane has been shown to improve survival in septic peritonitis in mice when applied as brief conditioning [10, 11], and has been discussed as an additional supportive treatment modality in sepsis [7].

The application of sevoflurane is strictly limited to controlled environments such as operating theaters or ICU due to its route of administration and anesthetic effects. To overcome this limitation of volatile anesthetics and to provide the protective effects to a broader target group, numerous attempts have been undertaken to encapsulate volatile anesthetics in lipid emulsions for intravenous administration [12]. Despite major efforts, none of these emulsions are currently used as part of our daily clinical routine. It would therefore be favorable to isolate the immunomodulating properties of volatile anesthetics in an injectable formulation, and to separate them from the anesthetic effect.

Interestingly, the presence of hexafluoro-2-propanol (HFIP), a water-soluble primary metabolite of the volatile anesthetic sevoflurane, has been associated with attenuated secretion of endotoxin-stimulated inflammatory mediators *in vitro* [13]. In addition, HFIP has been shown to improve 7-day survival in a model of septic

peritonitis in mice [14]. At present, no information is available on the underlying mechanisms of the beneficial inflammatory or immunomodulatory effect of HFIP. In particular, with regard to a future therapeutic administration, the effect also has to be reproducible in a different species and in different models of sepsis (type of sepsis induction; ICU-like conditions with sedation and mechanical ventilation). We therefore chose a well-established rat model of lipopolysaccharide (LPS)-induced inflammation that mimics the initial phase of sepsis [15] to study the early immunomodulatory effect of HFIP (**Fig. 1A**). We hypothesized that both HFIP and sevoflurane would attenuate the inflammatory response, reduce the invasion of effector cells, and decrease tissue damage evoked by endotoxin challenge. To uncover underlying molecular mechanisms of the effects provided by HFIP, we analyzed the gene expression profile of human microvascular endothelial cells (HMVEC) following stimulation with LPS (**Fig. 1B**). Special attention was paid to pathways downstream of the mammalian LPS receptor, Toll-like receptor 4 (TLR4) [16, 17], where we expected significant changes due to HFIP-mediated modulation of TLR4-activated pro-inflammatory responses.

Herein, we demonstrate in the rat model of acute endotoxemia that intravenous injection of HFIP reduces the levels of pro-inflammatory mediators in plasma and tissue, decreases subsequent neutrophil invasion, and attenuates apoptosis in internal organs. These effects are associated with suppression of NF-κB activation and expression of NF-κB-dependent transcripts.

EXPERIMENTAL PROCEDURES

Ethics statement – All animals were housed and handled in accordance with protocols approved by the local animal care and use committee, Zurich, Switzerland (No. 156/2010).

Wistar rats – Pathogen-free, adult male Wistar rats weighing 350 – 500g (Charles River, Sulzfeld, Germany) were used. The animals were allowed to acclimate for at least one week prior to initiation of procedures and were housed under a 12/12-hr light/dark regimen in standard cages at 22 ± 1°C. Food and water were supplied ad libitum.

Animal preparation – Anesthesia was induced with intraperitoneal sodium thiopental (100mg/kg; Pentothal, Ospedalia AG, Hünenberg, Switzerland). The left jugular vein was cannulated with a sterile 22-gauge catheter (BD Insyte; Becton Dickinson S.A., Madrid, Spain) for fluid administration and maintenance of anesthesia using continuous propofol infusion (Disoprivan 1%, AstraZeneca, Zug, CH; 10mg/kg/h). For animals of the sevoflurane group, intravenous application of propofol was stopped, replaced by a 30-min anesthesia with sevoflurane, and re-initiated thereafter. Arterial blood pressure was measured continuously with a sterile polyethylene catheter placed into the left carotid artery (pressure transducer; Spacelabs, Hertford, United Kingdom). Arterial blood samples (900 µl) were taken hourly for blood gas analyses and determination of inflammatory mediator levels. The blood volume was substituted by Ringer's lactate (B.Braun, Melsungen, Germany) in a 1:4 ratio (3.6 mL). A tracheotomy was performed and the rats were mechanically ventilated using the pressure-controlled mode (Servo Ventilator 300; Maquet, Solna, Sweden). Peak inspiratory pressure was 14 cm H2O, with a positive end-expiratory pressure of 3 cm H2O. The fractional inspired oxygen concentration (FiO2) was 0.6, inspiratory:expiratory ratio was 1:2, respiratory rate was 30/min and was corrected for normoventilation (arterial target CO2: 4.6-5.2 kPa) according to the blood gas analyzer. Body temperature was maintained at 37°C using a warming lamp.

Design of animal experiments – Thirty-six male Wistar rats were randomly assigned to blocks of two animals. The blocks were again randomized into the following

groups: I) LPS group (n=10), which received intravenous 1 mg/kg Escherichia coli endotoxin (LPS, E. coli endotoxin serotype 055:B5; Sigma-Aldrich, Buchs, Switzerland; dissolved at a concentration of 1 mg/mL in phosphate-buffered saline, (PBS) Kantonsapotheke Zurich, Zurich, Switzerland); II) LPS+HFIP group (n=7), which was treated identically to the LPS group with the additional administration of 67 mg/kg HFIP (Sigma-Aldrich, Buchs, Switzerland) in Ringer's lactate over 30 min after LPS injection; III) LPS+sevoflurane group (n=8), which was treated identically to the LPS group but with the additional administration of sevoflurane (Sevorane; Abott, Baar, Switzerland) using the Anesthetic Conserving Device (AnaConDa, Sedana Medical, Uppsala, Sweden) over 30 min after LPS injection [18] while propofol infusion was stopped and reinitiated after the 30min sevoflurane application; IV) CONTROL group with PBS instead of LPS (n=5); V) HFIP group in which animals received PBS and 67 mg/kg HFIP (n=5). Based on results from in vitro studies [19], we empirically decided to administer a dose of 67 mg/kg HFIP to rats, which corresponds to 0.39 mmol/kg total body weight (BW) or 4 mmol/L blood volume. This dose is comparable to previous experiments [14, 19] and significantly lower than the LD50 (around 180 mg/kg in mice when administered intravenously) [14]. To set these values in to the context of human subject exposures, 0.05 mmol/kg BW HFIP (primary metabolite) was measured after 3 hours of sevoflurane anesthesia [20]. In preliminary experiments, we administered 134 mg/kg (≈8 mmol/L blood) which is analogous to values obtained from in vitro experiments [13]. However, after bolus injection of the double dose, within two hours 100% mortality was observed in endotoxemic rats. One animal died due to technical reasons during the monitoring phase of the experimental procedure, which is why only 7 (and not 8) animals in the LPS+HFIP group were included in the analysis. The concentration of sevoflurane during the 30 min treatment was targeted at 1–2 vol% (0.5–1 minimum alveolar concentration, respectively) (LPS+sevoflurane group). All

animals received additional Ringer's lactate (30mL/kg) after injection of LPS over a time period of 1 hour. The animals were euthanized 6 hours after endotoxin infusion. Blood was drawn from the inferior vena cava. Finally, the lung (after bronchoalveolar lavage), the spleen, the liver, and the kidneys were snap-frozen in liquid nitrogen and tissue, bronchoalveolar lavage fluid (BALF) and plasma were stored at -80°C for isolation of RNA, cryosections, and determination of inflammatory cytokine levels (Fig. 1A).

Enzyme-linked immunosorbent assays (ELISA) used for assessment of inflammatory mediators – Sandwich ELISAs were performed according to the manufacturer's protocol, assessing monocyte chemoattractant protein 1 (MCP-1, BD Biosciences, San Diego, CA), interleukin 6 (IL-6, R&D Systems, Minneapolis, MN), and cytokine-induced neutrophil chemoattractant-1 (CINC-1, R&D Systems, Minneapolis, MN) in plasma and BALF. According to the manufacturer, the lower detection limits were 30 pg/mL for MCP-1, 30 pg/mL for IL-6, and 15 pg/mL for CINC-1.

Real-time PCR analysis of inflammatory mediators in tissue – Total RNA was isolated from liver, spleen, kidney and lung. After homogenization using 1.4 mm ceramic beads (MagNA Lyser Green Beads, Roche) and a Precellys homogenizer (Bertin Corp, Rockville, MD) for 2 x 30 sec at 6800 rpm, RNA was purified using the RNeasy minikit (Qiagen, Basel, CH) and cDNA was produced with 0.5 µg RNA in the HC cDNA Reverse Transcription Kit from (Qiagen, Basel, CH). Quantitative PCR was performed using the FastStart Universal Probe Master PCR Mix (Roche, Basel, CH), with labelled probes (Roche Probe Library, Basel, CH) and primers (Microsynth, Balgach, CH) designed for CINC, IL-6, MCP-1 and 18S. The final reaction volume of the assay was 15 µl and the PCR was performed on a LightCycler 480 Real Time PCR System (Roche, Basel, CH). The comparative Ct method was used for quantification of

the gene expression. The Cp values (Secondary Derivative Method, Roche) of the samples were normalized to the housekeeping gene (18S).

Determination of neutrophils in tissue – Frozen kidney and liver tissue was cut into 6 µm sections using the Cryostat HYRAX C60 (Zeiss, Jena, Germany). These sections were dried at room temperature for 1 hour and fixed with 4% paraformaldehyde for 10 min. After 3 washes with PBS, immunofluorescence staining on neutrophils was performed using a mouse anti-rat RP1 antibody (PharMingen, BD Biosciences, Allschwil, CH). After one hour incubation at 4°C, the sections were washed three times with PBS and subsequently incubated with the secondary antibody, Alexa Fluor 568 goat-anti-mouse IgG (Invitrogen, Life Technologies, CH) and diamidino-2-phenylindole (DAPI) for 1 hour at 4°C. The sections were scanned, using a Mirax Slidescanner (Zeiss, Feldbach, CH). Fluorescence intensity was quantified using the spotting method in the Imaris Image Processing and Analysis Software (Bitplane, Zurich, CH).

Measurement of caspase-3 activity in tissue – Caspases are cysteine proteases that play a key role in apoptotic signaling. These molecular scissors cleave their substrates after an aspartate residue. Kidney, lung, liver, and spleen tissue was isolated from rats and and immersed in ice-cold extraction buffer (25 mM 4-(2-hydroxyethyl)-1-piperazineethanesulfonic acid (HEPES), 5 mM MgCl2, 1 mM ethylene glycol tetraacetic acid (EGTA), 1 mM phenylmethanesulfonylfluoride (PMSF), 1 µg/mL protease inhibitor mix, all from Sigma, Allschwil, CH) with 1.4 mm ceramic beads (MagNA Lyser Green Beads, Roche, Switzerland) and homogenized using a Precellys homogenizer (2 x 30sec @ 6800 rpm). The supernatant was centrifuged at 20.000 rcf for 30 min at 4°C. Duplicate sets of protein samples (40 µg, determined by Bio-Rad protein assay) were incubated with fluorescent caspase-3 substrate Ac-DEVD-AMC (PeptaNova, Sandhausen, Germany) in extraction buffer with 1 mM DTT, and enzyme

activity was measured for 30 min at 350 nm (excitation) / 465 nm (emission) using a fluorescent spectrophotometer (Infinite M1000 Pro, Tecan, Männedorf, CH). As a positive control, 2 nM active human caspase-3 was added to the reaction (Institute of Biochemistry, University of Zurich, a gift from Dr. Heidi Roschitzki-Voser).

Determination of direct and indirect renal and hepatic tissue damage markers – Creatinine, blood urea nitrogen (BUN), aspartate transaminase (AST) and bilirubin were assessed using a biochemical analyzer (DRI-CHEM4000i, FUJIFILM, Japan). α1-microglobulin, a low molecular weight protein, was used as a marker for tubular function. Urine samples were collected at fixed time points; volumes and specific gravity were determined. All samples were centrifuged (1000 x g for 5 min), diluted 1:1000, and analyzed with a commercial α1-microglobulin ELISA (Hölzel Diagnostika GmbH, Cologne, Germany). The detection range was between 0.53 and 100 ng/mL.

Design of the experiments with human microvascular endothelial cells (HMVEC) – Human microvascular endothelial cells (CC-2815) derived from normal human microvascular blood vessels were purchased from Lonza (Verviers, Belgium) and cultured as described [13].. For gene expression analysis, cells were exposed for 6 hours to 20 µg/mL LPS (dissolved in PBS) from Escherichia coli serotype 055:B5 (Sigma-Aldrich, Buchs, Switzerland) to induce an inflammatory response (control cells were incubated with PBS) and co-exposed to 8 mmol/L HFIP (Sigma-Aldrich, Buchs, Switzerland) as in our previous study [13] (Fig. 1B).

Gene array analysis – Total RNA from HMVEC was extracted as described above. The quality of the isolated RNA was evaluated using NanoDrop ND 1000 (NanoDrop Technologies, Delaware, USA) and Bioanalyzer 2100 (Agilent, Waldbronn, Germany). Genome-wide RNA levels were assessed using the human gene expression SurePrint GE3 (8 × 60 K) microarray according to the manufacturer's protocol (Agilent). An Agilent Microarray Scanner (Agilent p/n G2505C) was used to measure the

fluorescence intensity emitted by the labeled targets. Raw data processing was performed using the Agilent Scan Control and Agilent Feature Extraction Software Version 10. In total, twelve samples with LPS- or PBS-stimulated HMVEC, from which 6 samples were treated with HFIP, were hybridized on microarrays. One sample of the LPS+HFIP group was lost due to technical error during the hybridization procedure. Data were deposited in NCBI's Gene Expression Omnibus (GEO).

Differential expression and pathway analysis – Differential expression analysis was performed using the limma package in R/Bioconductor (Fred Hutchinson Cancer Research Center, Seattle, WA) in which transcripts of genes were ranked according to fold-change and significance. Clustering of the selected genes was achieved using hierarchical clustering with Euclidean distance metric and average linkage to generate the hierarchical tree. Pathway analysis of significantly regulated genes was performed using MetaCore (GeneGo, St. Joseph, MI). MetaCore is a web-based software suite for functional analysis of experimental data, based on a manually curated database of human protein-protein, protein-DNA, and protein-compound interactions, as well as metabolic and signaling pathways.

Luciferase assay of AP-1 and NF-κB activity – Endothelial cells were grown in a 96-well plate to 70% confluence and starved overnight as described [19]. Diluted Plus Reagent (1:40 in Optimem, both from Invitrogen) was mixed with 100 ng DNA per well (Cignal Reporter Assay, Quiagen, Venlo, NL) and added to the same volume of diluted lipofectamine LTX (1:12.5 in Optimem, both from Invitrogen). Complex formation was allowed for 5 minutes at room temperature and cells were transfected for 4h in the incubator. Thereafter transfection media was replaced by growth media for 6h and changed back to serum-free media overnight. After exposure to 20 µg/ml LPS with or without 4 mM HFIP for 4 hours, luciferase activity was measured by Dual Luciferase Reporter Assay (Promega, Fitchburg, WI, USA) according to the manufacturer's

protocol. Activity of activator protein-1 (AP-1) and nuclear factor-kappa B (NF-κB) were corrected for transfection efficiency (firefly luciferase activity divided by renilla luciferase activity).

Influence of HFIP on the toll-like receptor 4 (TLR4) signaling pathway – After observing the gene expression profiles, we performed additional experiments in HMVEC using 20 µg/mL LPS, 10 nM phorbol-12-myristate-13-acetate (PMA) (Calbiochem©, Merck KGaA, Darmstadt, Germany) and 20 nM tumor necrosis factor-α (TNF-α) (R&D Systems, Abingdon, UK) as stimulants of an inflammatory response. Hexafluoro-2-propanol was administered at a concentration of 4 mmol/L. After 6 hours of exposure, we measured inflammatory mediator expression in supernatants using human IL-6 ELISA and human CINC-1 ELISA (both obtained from R&D Systems, Abingdon, UK).

Statistical analysis – Statistical analyses were performed with SPSS 20 (SPSS Inc., Chicago, IL) and OriginPro 8G (Origin Lab, Northampton, MA). Results in Fig. 2 and Fig. 5 are shown as mean ± standard deviation (SD). All other data are presented as boxplot figures with medians and quartiles. Whiskers represent 5% and 95% confidence intervals, * represent 1% and 99% confidence intervals. Linear regression was used to assess the influence on inflammatory mediator expression / tissue damage markers (dependent variables). The different treatment modalities (LPS, LPS+HFIP, LPS+sevoflurane, and HFIP) were included in the linear regression model as binary, independent predictors. If applicable, different measurement time points were addressed using a categorical, independent predictor variable. Control animals (or control cells, respectively) were used as reference category. All results are illustrated as B coefficients and corresponding 95% confidence intervals (Tables 1-8). Using binary independent predictor variables, the resulting B coefficients represent the averaged effect difference during the experiment in relation to untreated control animals or

control cells (reference category). For gene array and pathway analyses, we considered $p < 0.01$ as significant. For all other analyses a p-value < 0.05 was considered significant.

RESULTS

HFIP attenuates endotoxin-induced systemic inflammation – Systemic inflammation was evaluated hourly by assessment of a subset of surrogate markers in plasma which have proven to be prognostic factors for severity and outcome of sepsis, such as MCP-1, IL-6, and CINC-1 [21-23]. Stimulation with LPS provoked a rise in the plasma concentration of MCP-1, IL-6, and CINC-1 confirming the presence of a systemic inflammatory response in our model (Fig. 2A-C). Peak values were found 6 hours after administration of LPS: 5027 ng/mL for MCP-1, 101 ng/mL for IL-6, and 867 ng/mL for CINC-1. The LPS-induced secretion of MCP-1 and IL-6 protein decreased 43% and 72%, respectively, when animals were treated with HFIP (both $p<0.001$). Interleukin-6 concentration in HFIP-treated animals was comparable to control animals at the end of the experiment. In animals treated with HFIP slightly higher levels of CINC-1 were observed in plasma (mean difference +63ng/mL). Sevoflurane, the precursor of HFIP, reduced MCP-1 secretion by 47% ($p<0.001$) whereas IL-6 secretion was not affected by sevoflurane. Cytokine-induced neutrophil chemoattractant-1 was reduced by 76% ($p<0.001$) in endotoxemic animals treated with sevoflurane. Detailed changes in plasma concentrations of inflammatory mediators are listed in Table 1. Taken together, the data indicate that LPS-induced secretion of plasma inflammatory mediators is attenuated by HFIP and sevoflurane.

HFIP reduces the production inflammatory mediator mRNA in tissue – To examine whether HIFP and sevoflurane have a similar effect on production of inflammatory mediators in tissue as observed in the plasma, we determined mRNA

levels of MCP-1, IL-6, and CINC-1 in kidney, liver, lung and spleen (Tables 2-5). While these different tissues were assessed, a special focus was placed on the kidney and the liver as these organs are of particular interest in models of endotoxemia [15, 24]. In all organs, elevated mRNA levels of MCP-1, IL-6, and CINC-1 were observed upon stimulation with LPS, which is in accordance with the results from plasma measurements. While messenger RNA of all three inflammatory mediators was attenuated in all organs by HIFP treatment (all $p<0.01$), this effect could not be demonstrated for sevoflurane. In kidneys, sevoflurane decreased the expression of proinflammatory mediator mRNA, except for CINC-1, which remained unaffected (Table 2). In liver and spleen tissue, sevoflurane attenuated the LPS-stimulated elevation of all three inflammatory mediator mRNAs (Table 3 and 5). In the lung, sevoflurane reduced the amount of MCP-1 mRNA by 29% ($p<0.001$), but there was not a notable difference in IL-6 and CINC-1 mRNA levels (Table 3). Details of the changes in inflammatory mediator expression profiles are described in Tables 2-5. In summary, HFIP and to a lesser extent sevoflurane reduced LPS-induced mRNA production of proinflammatory mediators in kidneys, liver, lung, and spleen.

Decreased effector cell recruitment in kidney and liver in HFIP-treated animals – Dysfunction of the kidneys and the liver greatly contribute to the severity and outcome of systemic inflammation [25, 26]. Effector cells migrate towards the site of tissue injury along gradients of proinflammatory mediators. Excessive amounts of cytokines and an overshooting recruitment of activated effector cells might convert the normally beneficial effects of inflammation into a condition that is damaging to the host [27]. In order to examine the biological relevance of increased expression of inflammatory mediator mRNA in tissues, we quantified the amount of neutrophils in kidney and liver by immunofluorescence staining. In accordance with the observed elevation in inflammatory mediator mRNA, an increased number of neutrophils was

observed in the parenchyma after LPS stimulation (Tables 2 and 3). Administration of HFIP or sevoflurane reduced the LPS-induced neutrophil influx in both organs to levels comparable to that observed in control animals ($p<0.01$). These data illustrate that the decreased amount of inflammatory mediator mRNA, resulting from treatment with HFIP or sevoflurane, also translates into reduced effector cell recruitment.

HFIP-mediated attenuation of tissue damage and resulting effect on organ function – To estimate possible protective effects of the application of HFIP, we evaluated different tissue damage markers of the kidneys (Table 2), the liver (Table 3), the lung (Table 4) as well as the spleen (Table 5), focusing on apoptosis and necrosis. Whenever possible, we also tried to put the amount of tissue injury into context with the respective parameters of organ function. With regard to apoptosis, no difference in caspase-3 activity was observed in the kidneys in the different groups (overall p-value: 0.081) (Table 2). As a marker of tubular damage, α1-microglobulin was measured in urine. Increased α1-microglobulin after LPS stimulation was attenuated by both HFIP (-23%) and sevoflurane (-60%) suggesting a prevention of sepsis-induced tubular damage [28] (p-values<0.001). In septic animals, plasma creatinine and BUN concentrations were increased (by 24 mmol/L and by 3 mmol/L), which is consistent with there being impaired renal function. Administration of HFIP lowered the plasma creatinine concentration by 4 mmol/L ($p<0.05$), while BUN levels were not affected. In contrary to HFIP, sevoflurane aggravated the rise in creatinine (+17 mmol/L) and BUN concentration (+5 mmol/L) in comparison to animals treated with LPS alone ($p<0.001$). In liver tissue, LPS stimulation increased caspase-3 activity, and this effect was reduced by 48% and by 57% when animals received HFIP or sevoflurane, respectively ($p<0.01$, Table 3). Aspartate transaminase, a typical hepatocyte necrosis marker, was not influenced by LPS or by HFIP, but elevated levels were observed in animals receiving sevoflurane, independent of sepsis. In all animals, bilirubin concentrations were below

detection levels (<1.7 µmol/L). In the lung, caspase-3 activity was not affected by LPS stimulation, HFIP, or sevoflurane administration (overall p-value: 0.2, Table 4). Arterial oxygen partial pressures in animals remained unchanged with exception of the sevoflurane group, in which lower oxygen partial pressures were observed. Arterial oxygen saturation was >96% in all animals during the entire experiment. In the spleen, LPS induced a 2.4-fold increase in caspase-3 activity which was only slightly mitigated by HFIP but reached levels similar to that of control animals upon treatment with sevoflurane (Table 5). Taken together, HFIP and sevoflurane attenuated LPS-induced tissue injury. With regard to the kidneys, HFIP also attenuated LPS-induced impairment of renal function.

Stabilization of the blood pressure drop after HFIP administration in endotoxemic animals – In animals receiving LPS, mean arterial blood pressure (MAP) decreased from 146 mmHg to 60 mmHg over the duration of the experiment. The administration of HFIP stabilized the LPS-induced initial drop in MAP (Fig. 3): the blood pressure recovered after 2 hours, reaching a value of 102 mmHg at the end of the experiment ($p<0.001$, R^2: 0.458). This was not observed in sevoflurane treated animals where the mean arterial pressure dropped from 126 mmHg to 59 mmHg over the time of the experiment. During the 30 minutes of sevoflurane administration, a particularly pronounced decrease in MAP was observed which might be the result of an overlapping anesthetic and cardiovascular effect of sevoflurane and propofol. These results indicate that administration of HFIP prevents the LPS-induced drop in blood pressure.

Effects of HFIP on acid/base and electrolyte status – Independent of the injury and the treatment, only marginal differences in pH, pCO_2 and bicarbonate values were found (Table 6). In animals receiving sevoflurane, a small change in lactate level was measured (mean difference relative to control over 6 hours: +0.6 mmol/L, $p<0.001$). All LPS-treated animals had reduced bicarbonate levels, which was not reflected by a

decrease in the pH value. Only minimal changes in plasma electrolytes were measured, but worthy of note was the drop in chloride levels in the sevoflurane group by 12 mmol/L ($p<0.001$) (Table 6).

Gene expression analysis in human microvascular endothelial cells after exposure to HFIP – To gain insight into the underlying mechanism(s) of the immunomodulatory effect of HFIP, we performed a gene expression profile analysis of human microvascular endothelial cell (HMVEC) exposed to LPS [19]. A total of 42545 probes were expressed on the microarray. A heat map representation of the gene expression profiles in response to HFIP exposure is illustrated in Fig. 4A. LPS stimulation of HMVEC significantly affected 1925 gene transcripts of which 1022 were downregulated (284 with ≥2-fold change), and 903 upregulated (378 with ≥2-fold change). With the application of HFIP alone, 2746 transcripts significantly changed. Of these genes, 1406 genes were downregulated (444 with ≥2-fold change) and 1340 were upregulated (344 with ≥2-fold change). To illustrate the influence of HFIP on LPS-stimulated changes in gene expression, different Venn diagrams with intersections of transcripts showing a ≥2-fold change by both LPS and HFIP are shown in Fig. 4B and C. One hundred thirty nine of the 903 transcripts upregulated by LPS stimulation were downregulated by HFIP (48 of 378 transcripts with ≥2-fold change, Fig. 4B). Two hundred thirteen of 1022 transcripts downregulated by LPS stimulation were upregulated by HFIP treatment (59 of 284 transcripts with ≥2-fold change, Fig. 4C). Fifty-four transcripts that were already upregulated by LPS stimulation were further increased by HFIP (17 with ≥2-fold change), while 18 transcripts already downregulated by LPS stimulation were further decreased by the application of HFIP (1 with ≥2-fold change). We suspected important changes in gene expression induced by HFIP within the TLR4 pathway – the mammalian LPS sensor. To specifically address the postulated impact of HFIP on this particular pathway, an enrichment analysis using

the GeneGO MetaCore framework was performed. Downstream of TLR4 (Fig. S1), we found a significant downregulation in response to HFIP treatment in NF-κB and AP-1 dependent inflammatory-mediator expression in LPS-stimulated HMVEC (Fig. 4D). Based on these results, we assessed the influence of HFIP on both NF-κB and AP-1 in LPS-stimulated HMVEC using gene-reporter luciferase assays (Fig. 4E and 4F). Hexafluoro-2-propanol significantly reduced mean LPS-induced NF-κB activity by 73% ($p=0.005$, R^2: 0.424), wherease there was no effect of HFIP on AP-1 activity (overall $p=0.323$). Taken together, HFIP-induced immunomodulation in LPS-stimulated HMVEC is associated with reduced activity of NF-κB.

Localization of HFIP-immunomodulation within the toll-like receptor 4 (TLR4) signaling pathway – To further explore the mechanism and the site of action of HFIP on LPS-induced secretion of inflammatory mediators, the TLR4 pathway upstream of NF-κB was assessed. Endotoxin-induced inflammatory cytokine release is mediated by the TLR4 signaling pathway involving activation of interleukin-1 receptor-associated kinase 1/2 (IRAK 1/2), tumor necrosis factor (TNF) receptor-associated factor 6 (TRAF6), NF-kappa-beta-inducing kinase (NIK, MAP3K14), I kappa B kinases (IKK) which ultimately increase NF-κB activity (Fig. 5). In accordance with results from gene expression analysis, secretion of IL-6 and CINC-1 protein by LPS-stimulated HMVEC was attenuated when cells were treated with HFIP (Fig. 6A-B). To examine whether HFIP modulates the TLR4 pathway prior to NIK activation, we stimulated the cells with TNF-α instead of LPS. In this cascade, cytokine release is mediated through TRAF2, NIK and IKK, sharing NIK, IKK and NF-κB as common downstream elements (Fig. 5). Similar to that observed with LPS, HFIP reduced the expression of inflammatory mediators induced by TNF-α exposure (Fig. 6C-D, Table 7). The persistence of the HFIP effect suggests that HFIP may modulate signaling downstream of TRAF6 and

TRAF2. We thus next stimulated cells with PMA, which directly provokes cytokine secretion through stimulation of protein kinase C (PKC) [29, 30] and subsequent activation of IKK (Fig. 5). In response to PMA stimulation, HFIP reduced IL-6 and CINC-1 protein secretion (Fig. 6E-F, Table 8) suggesting that the modulation of inflammatory mediator secretion is located downstream of IKK.

DISCUSSION

We demonstrate HFIP-mediated attenuation of endotoxin-induced inflammatory processes in rats as reflected by decreases in surrogate markers of sepsis in plasma, decreased effector cell invasion into vital organs, and reduced tissue damage. In addition, administration of HFIP improved hemodynamic stability of the animals. Pathway analysis in an *in vitro* model of endotoxin-induced endothelial cell injury revealed that the attenuation of inflammatory mediator secretion is mediated by the attenuation of NF-κB activation and dependent transcript expression.

In recent work, we showed using the cecal ligation and puncture (CLP) model of sepsis that rats had a remarkable 7-day survival benefit when treated with HFIP [14]. While the study addressed important outcome parameters, the underlying mechanisms of HFIP that increased survival remained unclear. The present study therefore focused on the orchestration of the inflammatory response in an early phase of sepsis and demonstrated that HFIP decreased inflammatory mediator secretion and tissue damage in early endotoxemia. Differences in the effect of HFIP and sevoflurane might be explained by the different routes of administration, by different pharmacokinetics (long elimination half-life of HFIP versus fast wash-out of sevoflurane) [20], or by differences in the molecular structure (hydrophilicity, hydrophobicity). In LPS-stimulated animals receiving sevoflurane treatment, an initial drop in blood pressure was observed which is most likely due to the overlap of the two anaesthetics propofol

and sevoflurane (stopping the propofol infusion and starting the application of the volatile anaesthetic) in already impaired animals. The phase of low blood pressure with impaired organ perfusion would explain increased tissue damage markers such as BUN, creatinine, and AST as well as the lower arterial partial pressure of oxygen in the LPS+sevoflurane group. Despite this initial drop in blood pressure, the known anti-inflammatory effects of sevoflurane were confirmed in the present model of early phase endotoxemia [10, 31].

The more advanced states of sepsis are in particular characterized by a loss of key immune effector cells which die due to sepsis-mediated apoptosis [32] and ultimately lead to a failure of host defense mechanisms [33]. The prevention of sepsis-induced apoptosis therefore represents an interesting therapeutic target and has been shown to successfully ameliorate survival [33-35]. In the present article, we observed that HFIP and sevoflurane do not only modulate inflammatory mediator secretion, but also reduce apoptosis in liver and spleen of endotoxemic animals. Thus, HFIP and sevoflurane clearly differ from other therapeutic approaches aiming solely at the attenuation of the 'cytokine storm' in sepsis.

Gene expression and pathway analysis illustrated that HFIP-induced downregulation of inflammatory mediators was likely due to inhibition of NF-κB activation which is well known to play a crucial role in orchestrating the inflammatory response. Based on the results from the microarray analysis and gene-reporter luciferase assays, we assume that a major part of the anti-inflammatory effects of HFIP is mediated at the level of or downstream of the IKK complex. With reference to the results of our experiments with TNF-α and PMA must certainly be considered that amongst all these pathways flow equilibria might exist. There is, however, already limited data in support of NF-κB-dependent suppression of inflammatory mediators by volatile anesthetics [36, 37], which is in line with the present results.

While our findings suggest HFIP-induced protection may be clinically very important, these promising results should be tempered as successful translation may be limited due to important clinical features of human sepsis which are not adequately modelled by experiments in rodents. Furthermore, a single LPS injection is unlikely to mimic the inflammatory responses in human sepsis [15, 38], as highlighted in previous studies where therapeutic strategies that have been promising in endotoxin-based rodent models where unsuccessful in clinical practice [39, 40]. Potentially important factors determining survival such as genetic heterogeneity and gender variability of the inflammatory response, different time points of sepsis onset, as well as the presence of pre-existing comorbidities should also be addressed [15, 38, 41]. No model will ever fully reflect the complexity of human sepsis, but studies in intact organisms allow the observation of complex interactions between organ systems and analysis of underlying mechanisms. With regard to *in vivo* sepsis models, the best preclinical investigation consists of observations in a combination of different animal models comprising different species and different types of sepsis induction [38]. The strong anti-inflammatory effects of HFIP in our Wistar rat endotoxaemia model – complementary to our observation of improved survival in a CLP mouse model of sepsis [14] – strengthens the proposition of HFIP as a future treatment modality in sepsis. Being the chief metabolite of sevoflurane, a large number of patients have been exposed to low doses of HFIP, and data on the metabolism and pharmacokinetics of HFIP is available [20]. Presupposing even more detailed knowledge on the molecular mechanisms of its anti-inflammatory effects, the intravenous administration of HFIP may provide a novel therapeutic tool in the treatment of systemic inflammation and sepsis.

ACKNOWLEDGEMENTS

This study was supported by the Swiss National Science Foundation, Berne, Switzerland, Grant No. 320030_141216, by Unitectra (Technology Transfer Organization of the University of Zurich), Zurich, Switzerland) and the Swiss Society of Anaesthesiology and Reanimation (SGAR), Berne, Switzerland). We thank Fabian Aigner for his helpful support.

AUTHOR CONTRIBUTIONS

M.U., I.K.H, M.S., W.J.S. and B.B.S. designed research. M.U., I.K.H, M.H., C.B., B.R.Z., H.R., M.S. and R.S. did the experimental research. M.U., I.K.H., M.S., R.D.M. and B.B.S wrote the manuscript.

CONFLICT OF INTEREST

B.B.S. has received honoraria and research grants from Baxter and Abbott (no relation to the current study). B.B.S. has received research grants from the Transfer Office of the University of Zurich, Switzerland. M.U., I.K.H, W.J.S. and B.B.S are co-authors of the patent Injectable formulation for treatment and protection of patients having an inflammatory reaction or an ischemia reperfusion event, WO/2011/012283. M.H., R.R.S., C.B., B.R.Z., H.R., and M.S. declare no conflicts of interests.

REFERENCES

1. Lagu T, Rothberg MB, Shieh MS, Pekow PS, Steingrub JS, Lindenauer PK. Hospitalizations, costs, and outcomes of severe sepsis in the United States 2003 to 2007. Crit Care Med 2012; **40**:754-61.
2. Gaieski DF, Mikkelsen ME, Band RA, Pines JM, Massone R, Furia FF, Shofer FS, Goyal M. Impact of time to antibiotics on survival in patients with severe sepsis or septic shock in whom early goal-directed therapy was initiated in the emergency department. Crit Care Med 2010; **38**:1045-53.
3. Dellinger RP, Levy MM, Rhodes A, Annane D, Gerlach H, Opal SM, Sevransky JE, Sprung CL, Douglas IS, Jaeschke R, Osborn TM, Nunnally ME, Townsend SR, Reinhart K, Kleinpell RM, Angus DC, Deutschman CS, Machado FR, Rubenfeld GD, Webb SA, Beale RJ, Vincent JL, Moreno R. Surviving sepsis campaign: international guidelines for management of severe sepsis and septic shock: 2012. Crit Care Med 2013; **41**:580-637.
4. Landoni G, Fochi O, Tritapepe L, Guarracino F, Belloni I, Bignami E, Zangrillo A. Cardiac protection by volatile anesthetics. A review. Minerva Anestesiol 2009; **75**:269-73.
5. Beck-Schimmer B, Breitenstein S, Urech S, De Conno E, Wittlinger M, Puhan M, Jochum W, Spahn DR, Graf R, Clavien PA. A randomized controlled trial on pharmacological preconditioning in liver surgery using a volatile anesthetic. Ann Surg 2008; **248**:909-18.
6. Ferrero ME, Marni A, Gaja G, Salari PC, Tiengo M. Conditioning of immune response by anesthetics. Ann N Y Acad Sci 1992; **650**:331-6.
7. Kharasch ED, Coopersmith CM. Sleeping to Survive?: The Impact of Volatile Anesthetics on Mortality in Sepsis. Anesthesiology 2013.

8. De Conno E, Steurer MP, Wittlinger M, Zalunardo MP, Weder W, Schneiter D, Schimmer RC, Klaghofer R, Neff TA, Schmid ER, Spahn DR, Z'Graggen B R, Urner M, Beck-Schimmer B. Anesthetic-induced improvement of the inflammatory response to one-lung ventilation. Anesthesiology 2009; **110**:1316-26.

9. Julier K, da Silva R, Garcia C, Bestmann L, Frascarolo P, Zollinger A, Chassot PG, Schmid ER, Turina MI, von Segesser LK, Pasch T, Spahn DR, Zaugg M. Preconditioning by sevoflurane decreases biochemical markers for myocardial and renal dysfunction in coronary artery bypass graft surgery: a double-blinded, placebo-controlled, multicenter study. Anesthesiology 2003; **98**:1315-27.

10. Herrmann IK, Castellon M, Schwartz DE, Hasler M, Urner M, Hu G, Minshall RD, Beck-Schimmer B. Volatile anesthetics improve survival after cecal ligation and puncture. Anesthesiology 2013; **119**:901-6.

11. Lee HT, Emala CW, Joo JD, Kim M. Isoflurane improves survival and protects against renal and hepatic injury in murine septic peritonitis. Shock 2007; **27**:373-9.

12. Lucchinetti E, Schaub MC, Zaugg M. Emulsified intravenous versus evaporated inhaled isoflurane for heart protection: old wine in a new bottle or true innovation? Anesth Analg 2008; **106**:1346-9.

13. Urner M, Limbach LK, Herrmann IK, Muller-Edenborn B, Roth-Z'Graggen B, Schlicker A, Reyes L, Booy C, Hasler M, Stark WJ, Beck-Schimmer B. Fluorinated groups mediate the immunomodulatory effects of volatile anesthetics in acute cell injury. Am J Respir Cell Mol Biol 2011; **45**:617-24.

14. Herrmann IK, Castellon M, Schwartz DE, Hasler M, Urner M, Hu G, Minshall RD, Beck-Schimmer B. Intravenous application of a primary sevoflurane

metabolite improves outcome in murine septic peritonitis: first results. PLoS One 2013; **8**:e72057.

15. Doi K, Leelahavanichkul A, Yuen PS, Star RA. Animal models of sepsis and sepsis-induced kidney injury. J Clin Invest 2009; **119**:2868-78.
16. Beutler B. Tlr4: central component of the sole mammalian LPS sensor. Curr Opin Immunol 2000; **12**:20-6.
17. Medzhitov R, Preston-Hurlburt P, Janeway CA, Jr. A human homologue of the Drosophila Toll protein signals activation of adaptive immunity. Nature 1997; **388**:394-7.
18. Voigtsberger S, Lachmann RA, Leutert AC, Schlapfer M, Booy C, Reyes L, Urner M, Schild J, Schimmer RC, Beck-Schimmer B. Sevoflurane ameliorates gas exchange and attenuates lung damage in experimental lipopolysaccharide-induced lung injury. Anesthesiology 2009; **111**:1238-48.
19. Urner M, Limbach LK, Herrmann IK, Mueller-Edenborn B, Roth-Z'Graggen B, Schlicker A, Reyes L, Booy C, Hasler M, Stark WJ, Beck-Schimmer B. Fluorinated Groups Mediate the Immunomodulatory Effects of Volatile Anesthetics in Acute Cell Injury. Am J Respir Cell Mol Biol 2011; **45**:617-24.
20. Kharasch ED, Karol MD, Lanni C, Sawchuk R. Clinical sevoflurane metabolism and disposition. I. Sevoflurane and metabolite pharmacokinetics. Anesthesiology 1995; **82**:1369-78.
21. Bozza FA, Salluh JI, Japiassu AM, Soares M, Assis EF, Gomes RN, Bozza MT, Castro-Faria-Neto HC, Bozza PT. Cytokine profiles as markers of disease severity in sepsis: a multiplex analysis. Crit Care 2007; **11**:R49.
22. Damas P, Ledoux D, Nys M, Vrindts Y, De Groote D, Franchimont P, Lamy M. Cytokine serum level during severe sepsis in human IL-6 as a marker of severity. Ann Surg 1992; **215**:356-62.

23. Vermont CL, Hazelzet JA, de Kleijn ED, van den Dobbelsteen GP, de Groot R. CC and CXC chemokine levels in children with meningococcal sepsis accurately predict mortality and disease severity. Crit Care 2006; **10**:R33.

24. Hewett JA, Schultze AE, VanCise S, Roth RA. Neutrophil depletion protects against liver injury from bacterial endotoxin. Lab Invest 1992; **66**:347-61.

25. Guidet B, Aegerter P, Gauzit R, Meshaka P, Dreyfuss D. INcidence and impact of organ dysfunctions associated with sepsis*. Chest 2005; **127**:942-51.

26. Dear JW, Yasuda H, Hu X, Hieny S, Yuen PS, Hewitt SM, Sher A, Star RA. Sepsis-induced organ failure is mediated by different pathways in the kidney and liver: acute renal failure is dependent on MyD88 but not renal cell apoptosis. Kidney Int 2006; **69**:832-6.

27. Rittirsch D, Flierl MA, Ward PA. Harmful molecular mechanisms in sepsis. Nat Rev Immunol 2008; **8**:776-87.

28. O'Seaghdha CM, Hwang SJ, Larson MG, Meigs JB, Vasan RS, Fox CS. Analysis of a urinary biomarker panel for incident kidney disease and clinical outcomes. J Am Soc Nephrol 2013; **24**:1880-8.

29. Castagna M, Takai Y, Kaibuchi K, Sano K, Kikkawa U, Nishizuka Y. Direct activation of calcium-activated, phospholipid-dependent protein kinase by tumor-promoting phorbol esters. J Biol Chem 1982; **257**:7847-51.

30. Blumberg PM. Protein kinase C as the receptor for the phorbol ester tumor promoters: sixth Rhoads memorial award lecture. Cancer Res 1988; **48**:1-8.

31. Voigtsberger S, Lachmann RA, Leutert AC, Schlaepfer M, Booy C, Reyes L, Urner M, Schild J, Schimmer RC, Beck-Schimmer B. Sevoflurane Ameliorates Gas Exchange and Attenuates Lung Damage in Experimental Lipopolysaccharide-induced Lung Injury. Anesthesiology 2009; **111**:1238-48.

32. Hotchkiss RS, Tinsley KW, Swanson PE, Schmieg RE, Jr., Hui JJ, Chang KC, Osborne DF, Freeman BD, Cobb JP, Buchman TG, Karl IE. Sepsis-induced apoptosis causes progressive profound depletion of B and CD4+ T lymphocytes in humans. J Immunol 2001; **166**:6952-63.

33. Hotchkiss RS, Nicholson DW. Apoptosis and caspases regulate death and inflammation in sepsis. Nat Rev Immunol 2006; **6**:813-22.

34. Braun JS, Novak R, Herzog KH, Bodner SM, Cleveland JL, Tuomanen EI. Neuroprotection by a caspase inhibitor in acute bacterial meningitis. Nat Med 1999; **5**:298-302.

35. Hotchkiss RS, Chang KC, Swanson PE, Tinsley KW, Hui JJ, Klender P, Xanthoudakis S, Roy S, Black C, Grimm E, Aspiotis R, Han Y, Nicholson DW, Karl IE. Caspase inhibitors improve survival in sepsis: a critical role of the lymphocyte. Nat Immunol 2000; **1**:496-501.

36. Zhong C, Zhou Y, Liu H. Nuclear factor kappaB and anesthetic preconditioning during myocardial ischemia-reperfusion. Anesthesiology 2004; **100**:540-6.

37. Loop T, Scheiermann P, Doviakue D, Musshoff F, Humar M, Roesslein M, Hoetzel A, Schmidt R, Madea B, Geiger KK, Pahl HL, Pannen BH. Sevoflurane inhibits phorbol-myristate-acetate-induced activator protein-1 activation in human T lymphocytes in vitro: potential role of the p38-stress kinase pathway. Anesthesiology 2004; **101**:710-21.

38. Buras JA, Holzmann B, Sitkovsky M. Animal models of sepsis: setting the stage. Nat Rev Drug Discov 2005; **4**:854-65.

39. Zeni F, Freeman B, Natanson C. Anti-inflammatory therapies to treat sepsis and septic shock: a reassessment. Crit Care Med 1997; **25**:1095-100.

40. Laterre PF, Levy H, Clermont G, Ball DE, Garg R, Nelson DR, Dhainaut JF, Angus DC. Hospital mortality and resource use in subgroups of the

Recombinant Human Activated Protein C Worldwide Evaluation in Severe Sepsis (PROWESS) trial. Crit Care Med 2004; **32**:2207-18.

41. Kharasch ED, Coopersmith CM. Sleeping to survive?: The impact of volatile anesthetics on mortality in sepsis. Anesthesiology 2013; **119**:755-6.

FIGURE LEGENDS

Figure 1. Illustration of experimental setting: after a single injection of lipopolysaccharide (LPS), male Wistar rats were treated either with hexafluoro-2-propanol (HFIP) or with sevoflurane. An analysis of inflammatory mediators and tissue damage markers was performed (kidney, lung, liver, and spleen tissue) six hours after LPS injection (A). In human lung microvascular endothelial cells, gene expression and pathway analysis was performed after LPS and HFIP exposure (B). MCP-1=Monocyte chemoattractant protein-1, IL-6=interleukin-6, CINC-1=cytokine-induced neutrophil chemoattractant protein-1, BALF=bronchoalveolar lavage fluid, AST=aspartate transaminase, BUN=blood urea nitrogen.

Figure 2. HFIP and sevoflurane treatment attenuates plasma inflammatory mediator secretion in LPS-stimulated rats. Monocyte chemoattractant protein-1 (MCP-1), interleukin-6 (IL-6) and cytokine-induced neutrophil chemoattractant-1 (CINC-1) protein concentrations were determined hourly (0-6 hours, T0-T6) in plasma of lipopolysaccharide (LPS)-treated rats simultaneously exposed to either hexafluoro-2-propanol (HFIP) or sevoflurane (A, B, C). Values represent mean±SD.

Figure 3. HFIP induces a stabilization of mean arterial pressure (MAP) in endotoxemic animals. Using invasive blood pressure monitoring, we assessed mean arterial blood pressure every 10 minutes after injection of lipopolysaccharides (LPS) in male Wistar rats. Hexafluoro-2-propanol (HFIP) or sevoflurane was administered over 30 minutes (indicated by the blue bar). MAP of control and HFIP-treated animals is shown in supplementary Fig. S1.T0-T6=time point 0 to 6 hours. Values are mean±SD.

Figure 4. Hexafluoro-2-propanol (HFIP) reduces lipopolysaccharide-induced NF-kappa B activity in endothelial cells (HMVEC). Heat map illustrating the effect of lipopolysaccharide (LPS) stimulation on HMVEC mRNA expression in absence or presence of hexafluoro-2-propanol (HFIP) (A). Venn diagrams representing the number of transcripts regulated upon LPS-stimulation and those affected by HFIP (threshold=1, $p<0.01$) (B, C). Summary of significantly different transcripts within the toll-like receptor 4 (TLR4)-downstream network (gene symbol and probe name) in LPS-stimulated cells which underwent a treatment with HFIP (D). Gene activity of NF-kappa B and activator protein 1 (AP-1) in HMVEC measured by firefly luciferase assay (E, F). Whiskers represent 5% and 95% confidence intervals, * represent 1% and 99% confidence intervals. LPS=lipopolysaccharide, HFIP=hexafluoro-2-propanol, PBS=phosphate-buffered saline.

Figure 5. Schematic illustration of the TLR4-downstream / NF-κB upstream network. Lipopolysaccharide (LPS)-induced inflammatory cytokine release is mediated by the toll like-receptor 4 (TLR4) pathway involving activation of interleukin-1 receptor-associated kinase 1/2 (IRAK 1/2), tumor necrosis factor receptor-associated factor 6 (TRAF6), nuclear factor-κ B(NF-κB)-inducing kinase (NIK, MAP3K14), I kappa B kinases (IKK), and subsequent upregulation of NF-κB. Tumor necrosis factor-α (TNF-α)-related cytokine release is mediated through TNF receptor-associated factor 2 (TRAF2), NIK/MAP3K14, and IKK activating NF-κB. Phorbol-12-myristate-13-acetate (PMA) directly provokes cytokine secretion by activation of protein kinase C (PKC) through IKK and subsequent NF-κB activation.

Figure 6. Attenuation of inflammatory mediators by hexafluoro-2-propanol (HFIP) is mediated at the level of IKK or its downstream effectors. LPS-induced (A, B) and

TLR4-mediated (C, D) stimulation of Interleukin-6 protein (IL-6) and cytokine-induced neutrophil chemoattractant protein-1 (CINC-1) secretion in human microvascular endothelial cells (HMVEC). Exposure of HMVEC to PMA (E, F). MyD88=myeloid differentiation primary response 88; TRADD=tumor necrosis factor receptor-1-associated protein.

TABLES

Table 1. Linear regressions on plasma inflammatory mediators and hemodynamics

	LPS	LPS+HFIP	LPS+Sevoflurane	HFIP	Time	R^2
Cytokines						
MCP-1, ng/mL	**3329 (2679, 3979)** [a]	**1896 (1142, 2650)** [a]	**1748 (1070, 2427)** [a]	**-77 (-826, 672)** [a]	**404 (301, 506)** [a]	0.498
IL-6, ng/mL	**50 (35, 65)** [a]	14 (-3, 32)	**68 (52, 84)** [a]	1 (-17, 19)	**11 (9, 14)** [a]	0.476
CINC-1, ng/mL	**497 (321, 673)** [a]	**560 (356, 765)** [a]	120 (-63, 303)	79 (-127, 286)	**99 (71, 127)** [a]	0.333
Hemodynamics						
MAP, mmHg	**-19 (-23, -15)** [a]	1 (-4, 5)	**-26 (-31, -22)** [a]	0 (-4, 5)	**-2 (-2, -1)** [a]	0.458

The table contains the B coefficients (95% confidence intervals) of the linear regressions. The different treatments (LPS, LPS+HFIP, LPS+Sevoflurane, HFIP) were addressed using binary predictors, while the measurement time point was entered as categorical independent predictor. The resulting B coefficient represents the mean effect difference in relation to untreated control animals (reference category). MCP-1: monocyte chemoattractant protein-1, IL-6: interleukin-6 protein, CINC-1: cytokine-induced neutrophil chemoattractant-1 protein, MAP: mean arterial pressure, LPS: lipopolysaccharide, HFIP: hexafluoro-2-propanol. Significance: [a] $p<=0.001$, [b] $p<0.01$, [c] $p<0.05$.

Table 2. Linear regressions on inflammatory mediator, organ damage marker as well as organ function of the kidney

Marker	LPS	LPS+HFIP	LPS+Sevoflurane	HFIP	R^2
MCP-1 mRNA, n-fold	**527 (396, 658)** [a]	**257 (106, 408)** [b]	**280 (144, 416)** [a]	0 (-151,151)	0.785
IL-6 mRNA, n-fold	**580 (410, 749)** [a]	**366 (170, 562)** [a]	**390 (213, 566)** [a]	0 (-196, 195)	0.732
CINC-1 mRNA, n-fold	**71 (52, 90)** [a]	**36 (15, 58)** [b]	**71 (52, 91)** [a]	0 (-22, 22)	0.807
Neutrophils, cm^{-2}	**842 (453, 1231)** [a]	6 (-414, 426)	-46 (-496, 403)	11 (-361, 384)	0.710
Caspase-3 activity, a.u.	overall p-value = 0.081				
α-microglobulin, µg/mL	**168 (103, 234)** [a]	**127 (57, 196)** [a]	58 (-6, 122)	45 (-6, 122)	0.663
BUN, mmol/L	**3 (1, 5)** [a]	**4 (2, 6)** [a]	**8 (6, 10)** [a]	0 (-3, 2)	0.789
Plasma creatinine, mmol/L	**24 (4, 44)** [c]	20 (-3, 44)	**41 (20, 62)** [a]	-9 (-32, 14)	0.524

The table contains the B coefficients (95% confidence intervals) of the linear regression. The different treatments (LPS, LPS+HFIP, LPS+Sevoflurane, HFIP) were addressed using binary predictors, while the measurement time point was entered as categorical independent predictor. Using binary independent predictor variables, the resulting B coefficients represent the mean effect difference in relation to untreated control animals (reference category). MCP-1: monocyte chemoattractant protein-1, IL-6: interleukin-6 protein, CINC-1: cytokine-induced neutrophil chemoattractant-1 protein, BUN: blood urea nitrogen. LPS: lipopolysaccharide, HFIP: hexafluoro-2-propanol. Significance: [a] $p<=0.001$, [b] $p<0.01$, [c] $p<0.05$.

Table 3. Linear regressions on inflammatory mediator and organ damage marker of the liver

Marker	LPS	LPS+HFIP	LPS+Sevoflurane	HFIP	R^2
MCP-1 mRNA, n-fold	**19 (13, 26)** [a]	**13 (5, 20)** [a]	**10 (3, 16)** [b]	0 (-7, 7)	0.680
IL-6 mRNA, n-fold	**277 (213, 342)** [a]	**254 (180, 329)** [a]	**180 (112, 247)** [a]	0 (-75, 74)	0.826
CINC-1 mRNA, n-fold	**50 (38, 63)** [a]	**46 (32, 61)** [a]	11 (-2, 24)	0 (-15, 14)	0.840
Neutrophils, cm^{-2}.	**867 (323, 1411)** [b]	512 (-102, 1127)	37 (-619, 694)	417 (-138, 972)	0.458
Caspase-3 activity, a.u.	**4.4 (3.1, 5.7)** [a]	**2.3 (0.9, 3.8)** [b]	**1.9 (0.7, 3.2)** [b]	0.2 (-1.3, 1.6)	0.727
AST, U/L	116 (-42, 275)	17 (-165, 200)	**224 (59, 389)** [b]	62 (-121, 244)	0.280

The table contains the B coefficients (95% confidence intervals) of the linear regression. The different treatments (LPS, LPS+HFIP, LPS+Sevoflurane, HFIP) were addressed using binary predictors, while the measurement time point was entered as categorical independent predictor. Using binary independent predictor variables, the resulting B coefficients represent the mean effect difference in relation to untreated control animals (reference category). MCP-1: monocyte chemoattractant protein-1, IL-6: interleukin-6 protein, CINC-1: cytokine-induced neutrophil chemoattractant-1 protein. AST: Aspartate transaminase. LPS: lipopolysaccharide, HFIP: hexafluoro-2-propanol. Significance: [a] $p<=0.001$, [b] $p<0.01$, [c] $p<0.05$.

Table 4. Linear regressions on inflammatory mediator, organ damage marker as well as organ function of the lung

Marker	LPS	LPS+HFIP	LPS+Sevoflurane	HFIP	R^2
MCP-1 mRNA, n-fold	**116 (86, 146)** [a]	**82 (49, 114)** [a]	**82 (51, 114)** [a]	0 (-35, 35)	0.765
IL-6 mRNA, n-fold	**76 (48, 103)** [a]	**59 (29, 88)** [a]	**78 (49, 107)** [a]	0 (-31, 32)	0.677
CINC-1 mRNA, n-fold	**3 (2, 5)** [a]	**2 (1, 4)** [b]	**3 (1, 4)** [a]	0 (-2, 2)	0.565
BALF MCP-1 protein, ng/mL	**82.8 (56.4, 109.2)** [a]	**35.4 (7.2, 63.7)** [c]	19.5 (-8.0, 47.0)	0.7 (-29.8, 31.2)	0.687
BALF IL-6 protein, ng/mL	**6.3 (4.3, 8.3)** [a]	**5.9 (3.8, 8.1)** [a]	**2.6 (0.5, 4.7)** [c]	0.3 (-2.0, 2.7)	0.706
BALF CINC-1 protein, ng/mL	**5.3 (1.6, 9.0)** [b]	4.0 (-0.1, 8.0)	1.9 (1.9, 5.7)	-0.1 (-4.4, 4.1)	0.338
Caspase-3 activity, a.u.	overall p-value = 0.2				
pO2, kPa [d]	-2.3 (-4.7, 0.0)	-1.7 (-4.4, 0.9)	**-10.6 (-13.4, -7.8)** [a]	-1.0 (-3.7, 1.7)	0.405

The table contains the B coefficients (95% confidence intervals) of the linear regression. The different treatments (LPS, LPS+HFIP, LPS+Sevoflurane, HFIP) were addressed using binary predictors, while the measurement time point was entered as categorical independent predictor. Using binary independent predictor variables, the resulting B coefficients represent the mean effect difference in relation to untreated control animals (reference category). MCP-1: monocyte chemoattractant protein-1, IL-6: interleukin-6 protein-1, CINC-1: cytokine-induced neutrophil chemoattractant-1 protein. LPS: lipopolysaccharide, HFIP: hexafluoro-2-propanol, BALF: bronchoalveolar lavage fluid. Significance: [a] $p<=0.001$, [b] $p<0.01$, [c] $p<0.05$. [d] Regarding the pO2 levels, we also introduced the measurement time point as a predictor in the regression analysis: the b coefficient was -0.8 with a confidence interval of -1.5 to -0.1 ($p<0.05$).

Table 5. Linear regressions on inflammatory mediator and organ damage marker of the spleen

Marker	LPS	LPS+HFIP	LPS+Sevoflurane	HFIP	R^2
MCP-1 mRNA, n-fold	**49 (37, 62)** [a]	**41 (28, 54)** [a]	**43 (30, 56)** [a]	0 (-14, 14)	0.803
IL-6 mRNA, n-fold	**139 (105, 174)** [a]	**94 (57, 131)** [a]	**101 (65, 137)** [a]	0 (-40, 40)	0.784
CINC-1 mRNA, n-fold	**146 (100, 192)** [a]	**128 (79, 177)** [a]	**74 (26, 121)** [b]	0 (-53, 52)	0.711
Caspase-3 activity, a.u.	**2.4 (1.5, 3.2)** [a]	**2.1 (1.1, 3.1)** [a]	-0.5 (-1.4, 0.4)	-0.6 ()	0.778

The table contains the B coefficients (95% confidence intervals) of the linear regression. The different treatments (LPS, LPS+HFIP, LPS+Sevoflurane, HFIP) were addressed using binary predictors, while the measurement time point was entered as categorical independent predictor. Using binary independent predictor variables, the resulting B coefficients represent the mean effect difference in relation to untreated control animals (reference category). MCP-1: monocyte chemoattractant protein-1, IL-6: interleukin-6 protein, CINC-1: cytokine-induced neutrophil chemoattractant-1 protein. LPS: lipopolysaccharide, HFIP: hexafluoro-2-propanol. Significance: [a] $p<=0.001$, [b] $p<0.01$, [c] $p<0.05$.

Table 6. Linear regressions on acid/base status and plasma electrolytes

	LPS	LPS+HFIP	LPS+Sevoflurane	HFIP	Time	R^2
Acid/Base status						
pH	**0.08 (0.06, 0.12)** [a]	**0.09 (0.06, 0.12)** [a]	**0.09 (0.06, 0.11)** [a]	0.00 (-0.03, 0.03)	**-0.01 (-0.02, -0.01)** [a]	0.472
pCO2, kPa	**0.8 (0.4, 1.2)** [a]	**1.0 (0.5, 1.4)** [a]	**1.1 (0.6, 1.6)** [a]	0.4 (-0.1, 0.8)	**-0.4 (-0.5, -0.3)** [a]	0.416
HCO3-, mmol/L	**-2.1 (-3.1, -1.1)** [a]	**-2.1 (-3.2, -1.0)** [a]	**-2.2 (-3.2, -1.2)** [a]	0.6 (-0.4, 1.7)	**-0.8 (-1.1, -0.6)** [a]	0.426
Lactate, mmol/L	0.3 (0.0, 0.7)	0.0 (-0.4, 0.4)	**0.6 (0.3, 1.0)** [a]	-0.2 (-0.6, 0.2)	0.1 (0.0, 0.2)	0.181
Plasma electrolytes						
Potassium, mmol/L	0.1 (-0.2, 0.3)	**0.3 (0.0, 0.5)** [c]	0.2 (-0.1, 0.4)	-0.1 (-0.4, 0.2)	**0.2 (0.1, 0.2)** [a]	0.253
Sodium, mmol/L	0 (-1, 1)	**2 (1, 3)** [b]	**-2 (-3, -1)** [b]	0 (-1, 1)	**0 (0, 1)** [c]	0.306
Chloride, mmol/L	**2 (0, 3)** [b]	**3 (1, 4)** [a]	**-12 (-14, -10)** [a]	0 (-2, 1)	**1 (1, 2)** [a]	0.758

The table contains the B coefficients (95% confidence intervals) of the linear regression. The different treatments (LPS, LPS+HFIP, LPS+Sevoflurane, HFIP) were addressed using binary predictors, while the measurement time point was entered as categorical independent predictor. Using binary independent predictor variables, the resulting B coefficients represent the mean effect difference in relation to untreated control animals (reference category). LPS: lipopolysaccharide, HFIP: hexafluoro-2-propanol. Significance: [a] $p<=0.001$, [b] $p<0.01$, [c] $p<0.05$.

Table 7. Linear regression on inflammatory response in HMVEC after stimulation with tumor necrosis factor-α (TNF-α)

Marker	TNF-α	TNF-α +HFIP	HFIP	R^2
IL-6, pg/mL	**75 (58, 91)** [a]	**36 (19, 53)** [b]	-1 (-18, 16)	0.982
CINC-1, pg/mL	**3956 (2389, 5523)** [a]	**3160 (1592, 4727)** [a]	128 (-1439, 1695)	0.801

The table contains the B coefficients (95% confidence intervals) of the linear regression. The different treatments (TNF-α, TNF-α+HFIP, HFIP) were addressed using binary predictors. Using binary independent predictor variables, the resulting B coefficients represent the mean effect difference in relation to untreated control cells (reference category). CINC-1: cytokine-induced neutrophil chemoattractant-1 protein. IL-6: interleukin-6 protein. TNF-α: tumor necrosis factor α, HFIP: hexafluoro-2-propanol. Significance: [a] $p<=0.001$, [b] $p<0.01$.

Table 8. Linear regression on inflammatory response in HMVEC after stimulation with phorbol 12-myristate 13-acetate (PMA)

Marker	PMA	PMA+HFIP	HFIP	R^2
IL-6, pg/mL	**926 (715, 1138)** [a]	**813, (602, 1025)** [a]	-8 (-267, 252)	0.762
CINC-1, pg/mL	**1723 (1497, 1950)** [a]	**1341 (1115, 1567)** [a]	-117 (-394, 160)	0.906

The table contains the B coefficients (95% confidence intervals) of the linear regression. The different treatments (PMA, PMA+HFIP, HFIP) were addressed using binary predictors. Using binary independent predictor variables, the resulting B coefficients represent the mean effect difference in relation to untreated control cells (reference category). CINC-1: cytokine-induced neutrophil chemoattractant-1 protein. IL-6: interleukin-6 protein. PMA: phorbol 12-myristate-13-acetate, HFIP: hexafluoro-2-propanol. Significance: [a] $p<=0.001$.

Figure 1

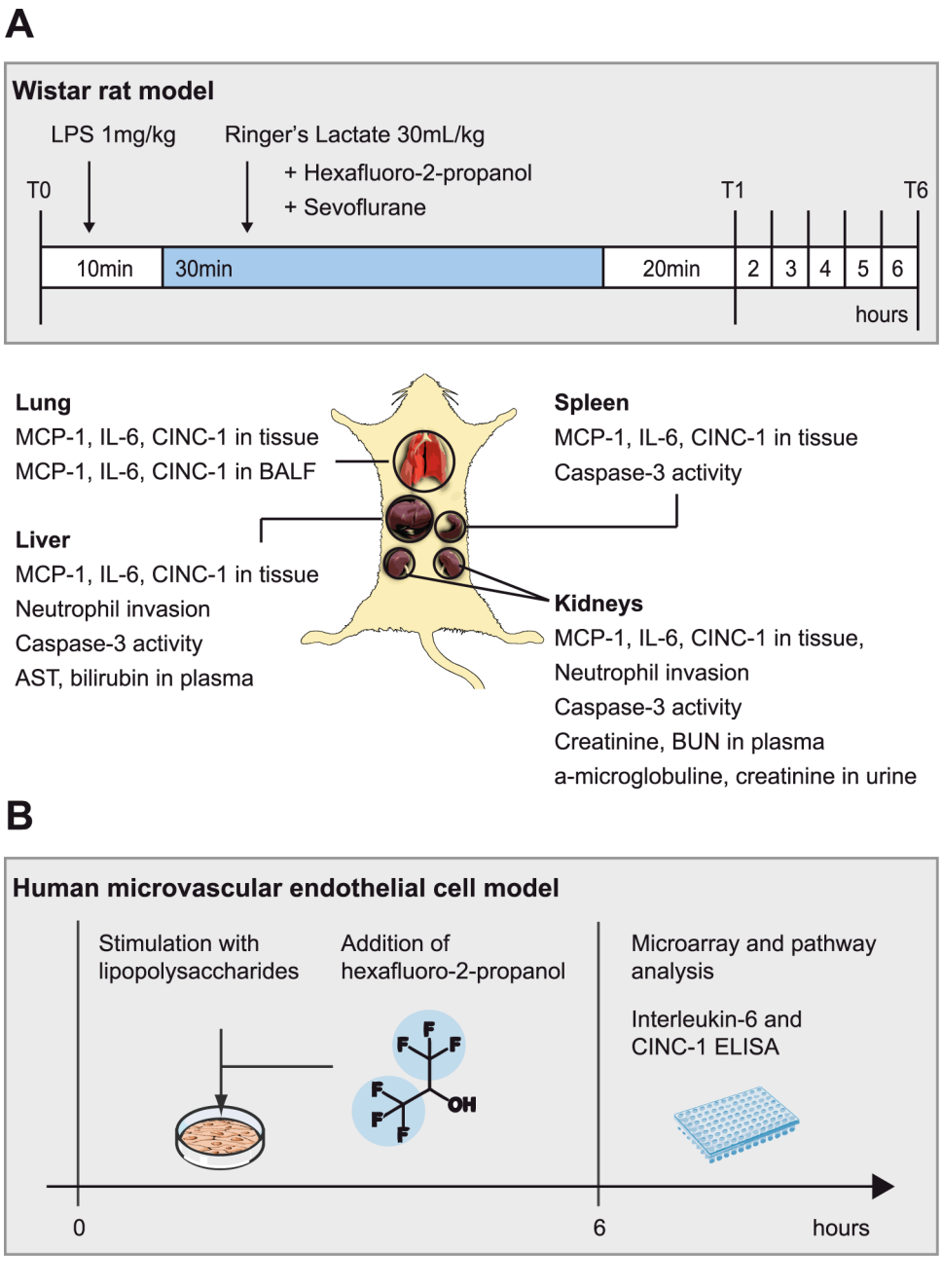
A
Wistar rat model
LPS 1mg/kg
Ringer's Lactate 30mL/kg
+ Hexafluoro-2-propanol
+ Sevoflurane
T0
T1
T6
10min
30min
20min
2
3
4
5
6
hours
Lung
MCP-1, IL-6, CINC-1 in tissue
MCP-1, IL-6, CINC-1 in BALF
Liver
MCP-1, IL-6, CINC-1 in tissue
Neutrophil invasion
Caspase-3 activity
AST, bilirubin in plasma
Spleen
MCP-1, IL-6, CINC-1 in tissue
Caspase-3 activity
Kidneys
MCP-1, IL-6, CINC-1 in tissue,
Neutrophil invasion
Caspase-3 activity
Creatinine, BUN in plasma
a-microglobuline, creatinine in urine
B
Human microvascular endothelial cell model
Stimulation with lipopolysaccharides
Addition of hexafluoro-2-propanol
Microarray and pathway analysis
Interleukin-6 and CINC-1 ELISA
F
F
F
F
F
OH
0
6
hours

Figure 2

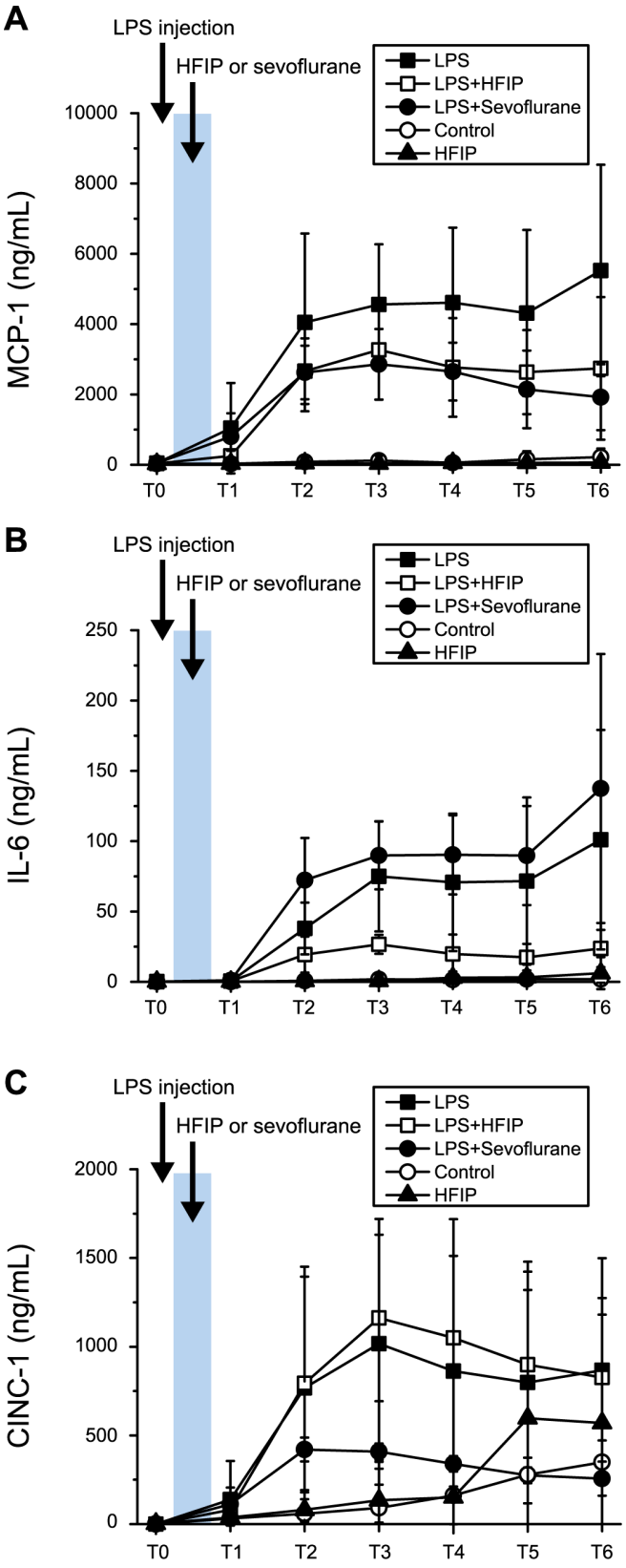

Figure 3

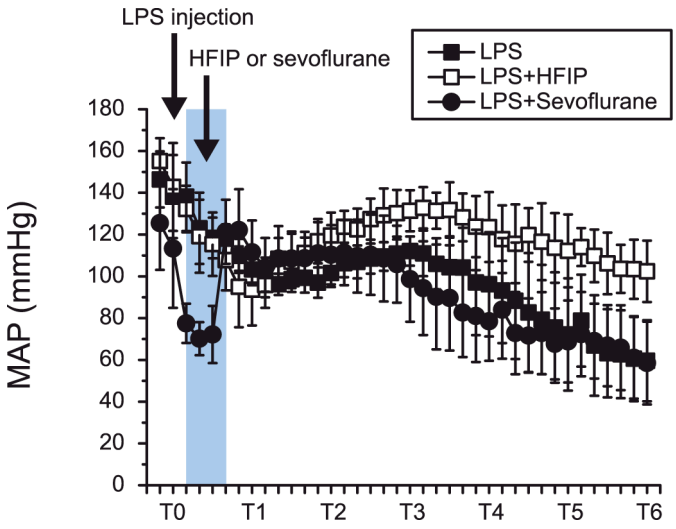
LPS injection
HFIP or sevoflurane
LPS
LPS+HFIP
LPS+Sevoflurane
MAP (mmHg)
180
160
140
120
100
80
60
40
20
0
T0
T1
T2
T3
T4
T5
T6

Figure 4

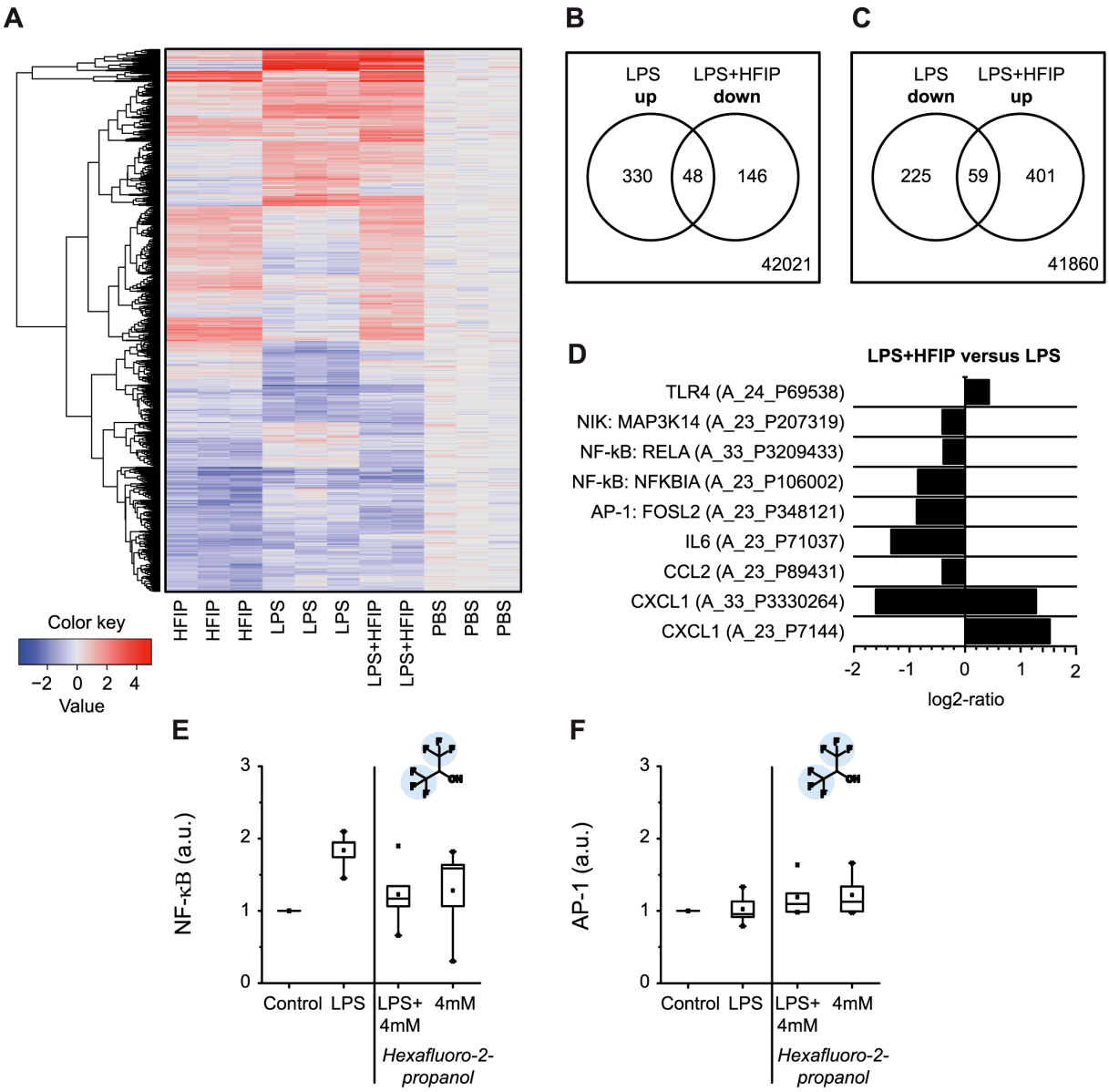
A
HFIP
HFIP
HFIP
LPS
LPS
LPS
LPS+HFIP
LPS+HFIP
PBS
PBS
PBS
Color key
−2 0 2 4
Value
B
LPS
up
LPS+HFIP
down
330
48
146
42021
C
LPS
down
LPS+HFIP
up
225
59
401
41860
D
LPS+HFIP versus LPS
TLR4 (A_24_P69538)
NIK: MAP3K14 (A_23_P207319)
NF-kB: RELA (A_33_P3209433)
NF-kB: NFKBIA (A_23_P106002)
AP-1: FOSL2 (A_23_P348121)
IL6 (A_23_P71037)
CCL2 (A_23_P89431)
CXCL1 (A_33_P3330264)
CXCL1 (A_23_P7144)
-2 -1 0 1 2
log2-ratio
E
NF-κB (a.u.)
0 1 2 3
Control LPS LPS+ 4mM 4mM
Hexafluoro-2-propanol
F
AP-1 (a.u.)
0 1 2 3
Control LPS LPS+ 4mM 4mM
Hexafluoro-2-propanol

Figure 5

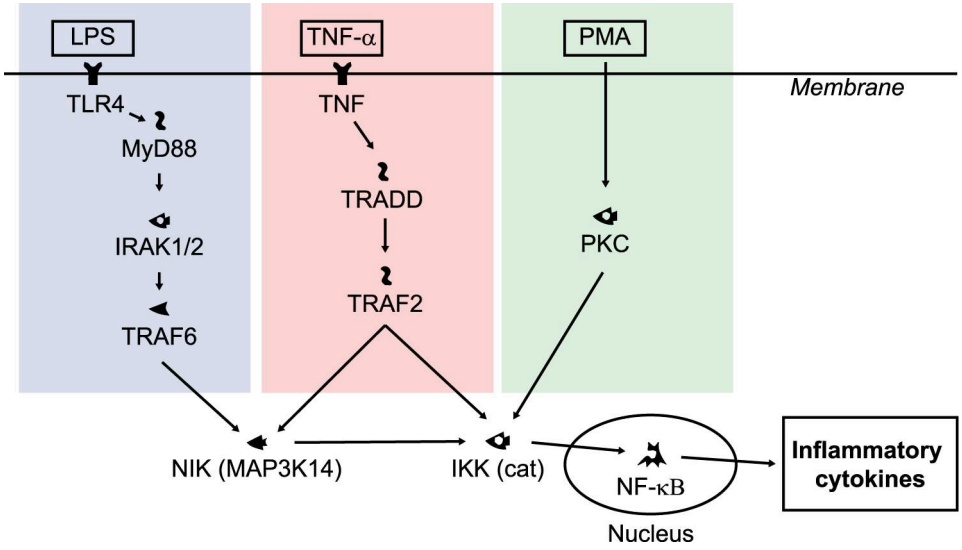
LPS
TNF-α
PMA
Membrane
TLR4
MyD88
IRAK1/2
TRAF6
TNF
TRADD
TRAF2
PKC
NIK (MAP3K14)
IKK (cat)
NF-κB
Nucleus
Inflammatory cytokines

Figure 6

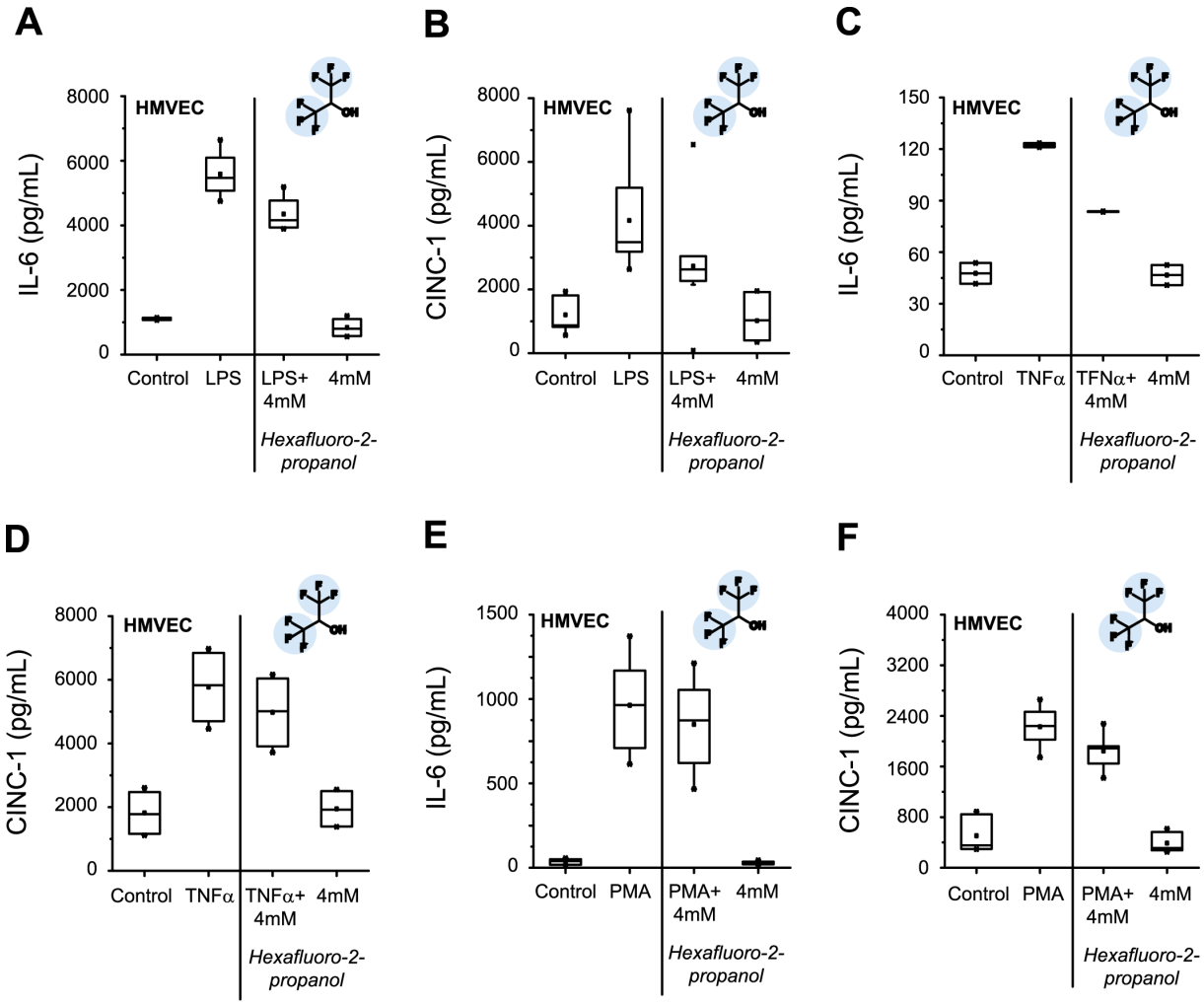
A
HMVEC
IL-6 (pg/mL)
8000
6000
4000
2000
0
Control
LPS
LPS+ 4mM
4mM
Hexafluoro-2-propanol
B
HMVEC
CINC-1 (pg/mL)
8000
6000
4000
2000
0
Control
LPS
LPS+ 4mM
4mM
Hexafluoro-2-propanol
C
HMVEC
IL-6 (pg/mL)
150
120
90
60
30
0
Control
TNFα
TFNα+ 4mM
4mM
Hexafluoro-2-propanol
D
HMVEC
CINC-1 (pg/mL)
8000
6000
4000
2000
0
Control
TNFα
TNFα+ 4mM
4mM
Hexafluoro-2-propanol
E
HMVEC
IL-6 (pg/mL)
1500
1000
500
0
Control
PMA
PMA+ 4mM
4mM
Hexafluoro-2-propanol
F
HMVEC
CINC-1 (pg/mL)
4000
3200
2400
1600
800
0
Control
PMA
PMA+ 4mM
4mM
Hexafluoro-2-propanol